Published in final edited form as:
Mol Microbiol. 2010 April ; 76(2): 517–534. doi:10.1111/j.1365-2958.2010.07119.x.

KRE genes are required for β-1,6-glucan synthesis, maintenance of capsule architecture and cell wall protein anchoring in *Cryptococcus neoformans*

Nicole M. Gilbert[1], **Maureen J. Donlin**[1,2], **Kimberly J. Gerik**[3], **Charles A. Specht**[4], **Julianne T. Djordjevic**[5], **Christabel F. Wilson**[5], **Tania C. Sorrell**[5], and **Jennifer K. Lodge**[3,*]

[1]Edward A. Doisy Department of Biochemistry and Molecular Biology, Saint Louis University School of Medicine, MO 63104, USA

[2]Department of Molecular Microbiology and Immunology, Saint Louis University School of Medicine, MO 63104, USA

[3]Department of Molecular Microbiology and Immunology, Washington University School of Medicine, MO, 63110, USA

[4]Department of Medicine, University of Massachusetts, MA, 01605, USA

[5]Centre for Infectious Diseases and Microbiology, ICPMR and Westmead Millennium Institute, University of Sydney at Westmead Hospital, NSW, 2145, Australia

Summary

The polysaccharide β-1,6-glucan is a major component of the cell wall of *Cryptococcus neoformans*, but its function has not been investigated in this fungal pathogen. We have identified and characterized seven genes, belonging to the *KRE* family, which are putatively involved in β-1,6-glucan synthesis. The H99 deletion mutants *kre5*Δ and *kre6*Δ*skn1*Δ contained less cell wall β-1,6-glucan, grew slowly with an aberrant morphology, were highly sensitive to environmental and chemical stress and were avirulent in a mouse inhalation model of infection. These two mutants displayed alterations in cell wall chitosan and the exopolysaccharide capsule, a primary cryptococcal virulence determinant. The cell wall content of the GPI-anchored phospholipase B1 (Plb1) enzyme, which is required for cryptococcal cell wall integrity and virulence, was reduced in *kre5*Δ and *kre6*Δ*skn1*Δ. Our results indicate that *KRE5*, *KRE6* and *SKN1* are involved in β-1,6-glucan synthesis, maintenance of cell wall integrity and retention of mannoproteins and known cryptococcal virulence factors in the cell wall of *C. neoformans*. This study sets the stage for future investigations into the function of this abundant cell wall polymer.

Keywords

phospholipase; chitosan; chitin deacetylase

Introduction

Cryptococcus neoformans is an opportunistic fungal pathogen that causes potentially fatal meningoencephalitis in immunocompromised individuals, especially patients with AIDS. The cryptococcal cell wall is an essential organelle, vital for maintaining cell morphology

*Correspondence to lodgejk@wustl.edu; Tel. 314-286-2125;, Fax: 314-362-7325.

and integrity. Since it is essential in fungi and its components are absent from mammalian host cells, the cell wall is an attractive target for antimicrobial therapies. The cryptococcal cell wall is composed of α- and β-linked glucans, chitin and its deacetylated derivative chitosan, and mannoproteins. In contrast to ascomycetes such as *Saccharomyces cerevisiae* and *Candida albicans*, in which β-1,3-glucan predominates (Klis *et al*., 2001; Klis *et al*., 2006), β-1,6-glucan is the most prevalent cell wall β-linked glucan molecule in *C. neoformans* (James *et al*., 1990). Despite its abundance, the function of β-1,6-glucan in the cryptococcal cell wall has not previously been investigated.

To date, no β-1,6-glucan synthase protein has been identified in any fungal species, which is in stark contrast to the well-characterized synthase enzymes of other major cell wall components (Araki and Ito, 1975; Shematek *et al*., 1980; Shaw *et al*., 1991; Ziman *et al*., 1996; Hochstenback *et al*., 1998). However, large-scale genetic screens have identified several *S. cerevisiae* proteins required for normal levels of cell wall β-1,6-glucan. These include Kre1p, Kre9p, Kre11p, Knh1p, Kre5p, and the functional homologs Kre6p and Skn1p. Several are localized along the secretory pathway, leading to the idea that β-1,6-glucan synthesis may involve intracellular events (reviewed in Shahinian and Bussey, 2000). A recent report using *in silico* analysis determined *KRE1*, *KRE9*, *KRE11*, and *KNH1* are Ascomycete-specific, suggesting that these genes are not essential for the synthesis of β-1,6-glucan and are more likely involved in modification of the polymer (Ruiz-Herrera *et al*., 2008). *KRE5* contains a COOH-terminal ER-retention sequence and shares some sequence homology to mammalian UDP-glucose glycoprotein glycosyltransferases (UGGTs) (Meaden *et al*., 1990) while the *KRE6*/*SKN1* genes encode *cis*-Golgi type II transmembrane proteins sharing 66% amino acid identity (Roemer *et al*., 1994). In *S. cerevisiae*, deletion of *KRE5* results in complete loss of alkali-insoluble cell wall β-1,6-glucan while disruption of *KRE6* reduced β-1,6-glucan levels to half of that measured from wild type cells (Roemer and Bussey, 1991). Loss of *SKN1* alone had no effect but its deletion further decreased the β-1,6-glucan levels in a *kre6 null* background (Roemer *et al*., 1993). The decrease in β-1,6-glucan in these mutants adversely affects growth, morphology and cell integrity (Meaden *et al*., 1990; Roemer and Bussey, 1991). Deletion of *KRE5* in the fungal pathogen *C. albicans* had similar effects and resulted in decreased virulence, highlighting a potential role for this gene and β-1,6-glucan in fungal pathogenesis (Herrero *et al*., 2004).

In several fungal species, the majority of cell wall proteins are attached to β-1,6-glucan via a remnant of their glycosylphosphatidylinositol (GPI) anchor (Kapteyn *et al*., 1996; de Groot *et al*., 2007; Yin *et al*., 2005). Homology searches of the *C. neoformans* genome predicted that there are 55 GPI-anchored proteins (Levitz and Specht, 2006), 16 of which have been identified by mass spectrometry in the extracellular proteome (Eigenheer *et al*., 2007). Among these proteins were three chitin deacetylases (Cdas), responsible for the enzymatic conversion of chitin to chitosan (Baker *et al*. 2007). The cryptococcal virulence factor phospholipase B1 (Plb1) is also GPI-anchored and concentrated in the cell wall (Djordjevic *et al*. 2005; Siafakas *et al*. 2006; Siafakas *et al*. 2007). Digestion of wild type cryptococcal cells with β-1,3-glucanase released Plb1 linked to β-1,6-glucan polymer, suggesting covalent attachment between Plb1 and β-1,6-glucan. Plb1 is also secreted from the *C. neoformans* surface during infection and facilitates tissue invasion. The cell wall appears to be a source of Plb1 as β-1,6-glucan was detected on the secreted enzyme (Siafakas *et al*. 2007).

In this study we have used gene deletion to investigate the role of seven genes of the *KRE* family, for their potential role in β-1,6-glucan synthesis in *C. neoformans*. We demonstrate that deletion of *KRE5* alone or *KRE6* and *SKN1* in combination results in the loss of cell wall β-1,6-glucan, accompanied by disruption of growth, morphology, cell wall integrity and virulence. Additionally, two important virulence factors, the exopolysaccharide capsule and

the GPI anchored mannoprotein Plb1, as well as cell wall chitosan, are altered in these mutants.

RESULTS

C. neoformans encodes seven potential β-1,6-glucan synthesis-related genes

We used a homology-based approach to identify genes in *C.neoformans* potentially required for β-1,6-glucan synthesis, utilizing *S. cerevisiae* proteins cited in the literature as being involved in this process (Shahinian and Bussey, 2000). The proteins Kre1p, Kre11p and Kre9p/Knh1p paralogs, all associated with β-1,6-glucan synthesis in *S. cerevisiae*, had no apparent homologs in the H99 genome. This is in agreement with a similar analysis in the fungal plant pathogen *Ustilago maydis* that determined these genes are specific to ascomycetes and absent from basidiomycetes (Ruiz-Herrera *et al*. 2008). Our results provide further support for the proposal that the mechanism of β-1,6-glucan synthesis in *C. neoformans* and other basidiomycetes may be distinct from that in *S. cerevisiae* and ascomycetes, or that the proteins have significantly diverged throughout the evolutionary process.

This search did yield one potential cryptotoccal homolog of *S. cerevisiae* Kre5p and six of the Kre6/Skn1 proteins (Table 1). The *C. neoformans* Kre6/Skn1 proteins were all quite similar to their *S. cerevisiae* homologs, varying from 38 – 48% identity and 53 – 61 % similarity at the amino acid level (Table 2). The *C. neoformans* homologs were more similar to each other, with 45 – 69% identity and 59 – 81 % similarity (Table 3). This clustering of the *C. neoformans* Kre6/Skn1 proteins is evident in the phylogenetic tree generated from an alignment of all the Kre6/Skn1 homologs from *S. cerevisiae*, *C. neoformans* and *C. albicans*, shown in Figure 1. A domain analysis using InterProScan revealed that the Kre6/Skn1 proteins from *S. cerevisiae, C. albicans* and the Skn1p, Kre6p, Kre61p and Kre62p from *C. neoformans* shared the same domains, domain number and domain organization (Fig. 2). The Kre63p and Kre64p have the major Skn1 domain, but neither has a transmembrane spanning domain and Kre64p has only 1 concanavalin A while Kre63p has none. This would suggest that the Kre6p, Skn1p, Kre61p and Kre62p may be functionally redundant in *C. neoformans*.

Ruiz-Herrera *et al*. (2008) reported a similar expansion of the *KRE6/SKN1* gene family in *U. maydis*. To determine whether this was true of other basiomycetes we conducted a BLASTp analysis of the NR database using *C. neoformans* Kre6 protein as the query and limiting the search to either basidiomycetes or ascomycetes species. We utilized the taxonomy report features to identify the number of possible Kre6 homologs in each species, using a cut-off of $E \leq 1e^{-100}$. Within the basidiomycetes, we found expanded families of Kre6/Skn1 like proteins in 3 species. *Ustilago maydis* had 7 homologs with E-values ranging from $6e^{-135}$ to $4e^{-116}$, all of which contained an Skn1 and concanavalin A-like lectin/glucanase domains. *Laccaria bicolor* had 6 homologs with E-values ranging from $8e^{-146}$ to $1e^{-119}$. *Coprinopsis cinerea* had 7 homologs with E-values ranging from $1e^{-139}$ to $3e^{-110}$. In all cases, the region of similarity covered the entire Skn1 domain of the *C. neoformans* Kre6 protein. We examined 25 ascomycetes species, almost all of which had only 1–2 potential Kre6/Skn1 homologs. This initial blast analysis suggests that an expanded family of Kre6-like proteins might be a distinguishing features of basidiomycetes compared to ascomycetes, although the number of basidomycete genomes is limited at this time.

KRE gene expression is temperature-regulated during vegetative growth

The existence of multiple *KRE6* homologs suggests functional redundancy between these genes and that they may be differentially expressed under different biological conditions.

We used northern blot analysis to determine the expression profiles of the putative *KRE5* and the *KRE6*/*SKN1* homologs during vegetative growth. *KRE5, SKN1, KRE6* and *KRE61* were expressed at 30°C (Fig. 3), whereas growth at 37°C showed comparatively higher expression of *KRE6* and *SKN1* but lower *KRE61* expression. The remaining genes displayed no detectable expression at either temperature. These data lead to the hypothesis that *KRE6* and *SKN1* may be functionally redundant, especially during growth at 37°C.

Generation of deletion strains

We generated targeted single deletions of *KRE5, SKN1* and each of the *KRE6/SKN1* genes using homologous recombination in the *C. neoformans* H99 strain. We also attempted to generate the various double deletion combinations of *KRE6, KRE61* and *SKN1*, as they were the only *KRE6/SKN1* genes with detectable mRNA expression during vegetative growth. Surprisingly, we were unable to obtain *kre61*Δ*skn1*Δ isolates despite multiple attempts at deleting either gene in the opposite single deletion background. One transformation yielded viable colonies, but Southern blot analysis reveled the presence of both the NAT marker deletion cassette and the deleted region, indicating a gene duplication event may have occurred prior to transformation (data not shown). This evidence, although not conclusive, is consistent with synthetic lethality between *KRE61* and *SKN1*, but such a possibility must be explored further in a mating competent background strain.

The phenotypes of the *kre61*Δ, *kre62*Δ, *kre63*Δ, *kre64*Δ, and *skn1*Δ strains were indistinguishable from wild type in all experiments tested. This is somewhat unexpected for *kre61*Δ, as *KRE61* mRNA was detectable at both 30 and 37 °C. However, the phenotypes obtained for the *kre62*Δ, *kre63*Δ and *kre64*Δ strains are consistent with the northern analysis, which detected no expression of *KRE62, KRE63* or *KRE64* mRNA.

The *kre5*Δ, *kre6*Δ, *kre6*Δ*kre61*Δ and *kre6*Δ*skn1*Δ mutants demonstrated abnormal phenotypes, as described below. The synthetic phenotypes displayed by the *kre6*Δ*skn1*Δ mutant, although not conclusive evidence, suggests functional redundancy between these genes. In multiple attempts to complement the *kre5*Δ and *kre6*Δ*skn1*Δ mutations, the mutant strains were completely recalcitrant to transformation either by biolistics or electroporation, yielding no viable colonies. Therefore, independent deletion isolates were used for analysis.

KRE5, KRE6 and SKN1 are involved in β-1,6-glucan synthesis in C. neoformans

We further tested our hypothesis that proteins expressed from the *KRE* genes are involved in β-1,6-glucan synthesis in *C. neoformans* by analyzing β-1,6-glucan in cell walls prepared from each of the deletion mutants. Cell wall polysaccharides can be separated into an alkali-soluble fraction and a fraction that is alkali-insoluble due to the cross-linking of the polysaccharides to insoluble chitin polymers (Hartland *et al*. 1994). We initially analyzed the alkali-soluble cell wall material by dot blotting, using a polyclonal anti-β-1,6-glucan antiserum as described by Maneesri *et al*. (2005). Although this assay is not quantitative for the level of β-1,6-glucan in the cell wall, the assay does demonstrate qualitative differences between the overall levels of the polymer among the strains. We confirmed this antibody is specific for β-1,6-glucan in *C. neoformans* by demonstrating that pustulan, a purified β-1,6-glucan, was the only polysaccharide that significantly competed for antibody binding to wild type alkali-soluble cell wall material (Fig. 4A). Alkali-soluble β-1,6-glucan was absent from *kre5*Δ and *kre6*Δ*skn1*Δ using this method while *kre6*Δ, *skn1*Δ and other deletion strains had levels similar to those of wild type (Fig. 4B, Suppl. Fig 1).

These results indicated that *kre5*Δ and *kre6*Δ*skn1*Δ are deficient in cell wall β-1,6-glucan. An alternative explanation was that β-1,6-glucan levels are unchanged in the mutants, but the polymer had shifted to the insoluble fraction. Such phenomena have been observed for

other cell wall mutants (Reese *et al*., 2007). Therefore, we further analyzed the alkali-insoluble fractions by digesting with purified chitinase to release glucans into the soluble fraction. As shown in Fig. 4C, this treatment released β-1,6-glucan from the alkali-insoluble fraction of wild type cells. However, no β-1,6-glucan was released from the corresponding fractions of *kre5*Δ or *kre6*Δ*skn1*Δ cells. These results indicated that loss of *KRE5* or *KRE6* and *SKN1* causes a decrease in the level of cell wall β-1,6-glucan.

Disruption of KRE5 or KRE6 and SKN1 alters cell morphology

Since the cell wall is a primary determinant of cell shape, we established whether alterations in β-1,6-glucan levels in *kre5*Δ or *kre6*Δ*skn1*Δ would alter cell morphology. Mutant strains were stained with the general cell wall stain Pontamine Fast Scarlet (Hoch *et al*., 2005), and examined by both light and fluorescent microscopy. The cell morphology and pattern of pontamine staining obtained for the *skn1*Δ, *kre6*Δ, *kre61*Δ, *kre62*Δ, *kre63*Δ, *kre64*Δ and *kre6*Δ*kre61*Δ deletion strains were indistinguishable from that of wild type (Suppl. Fig. 2). However, Fig. 5 shows the *kre5*Δ and *kre6*Δ*skn1*Δ cells were enlarged compared to wild type cells, formed clumps and contained large intracellular vacuole/vesicle structures. Multiple buds were present, resulting in chains of cells formed by incomplete separation of daughter cells from the mother cell.

Loss of KRE5 or KRE6 and SKN1 affects sensitivity to high temperature and cell wall inhibitors but not antifungal agents

The deletion mutants were tested for sensitivity to conditions that challenge cell wall integrity, including increased temperature and various cell wall inhibiting agents. Calcofluor white binds chitin fibrils and disrupts their assembly (Roncero and Durán 1985); caffeine interferes with cell wall integrity-related signal transduction pathways (López-Sáez *et al*., 1982); sodium dodecyl sulfate (SDS) disrupts the plasma membrane and lyses cells with membrane or cell wall defects; Congo red binds β-glucans and inhibits the microfibril assembly of the cell wall (Roncero and Durán, 1985). The *kre5*Δ and *kre6*Δ*skn1*Δ strains grew slowly at 30°C and growth was further inhibited at 37°C (Fig. 6A). This temperature sensitivity was partially rescued by the addition of 1M sorbitol, commonly used as an osmotic stabilizer, in the medium, with the growth of *kre5*Δ being more fully restored than that of *kre6*Δ*skn1*Δ (Fig. 6A). Loss of *KRE5* or both *KRE6* and *SKN1* resulted in increased sensitivity to all cell wall inhibitors tested (Fig. 6B). The *kre6*Δ mutant was mildly sensitive to 0.03% SDS, and this sensitivity was rescued by complementation with the wild type gene (Fig. 6B). The *kre6*Δ*kre61*Δ double deletion strain displayed only the SDS sensitivity observed for *kre6*Δ (Fig. 6B). Deletion of the five remaining *KRE6/SKN1* homologs individually did not cause an observable increase in sensitivity under any of the conditions tested (Suppl. Fig. 3).

The *kre5*Δ and *kre6*Δ*skn1*Δ mutants were also tested for sensitivity to the antifungal compounds fluconazole, voriconazole and caspofungin. Fluconazole and voriconazole disrupt production of ergosterol in the fungal plasma membrane and caspofungin inhibits β-1,3-glucan synthesis. Neither mutant had altered sensitivities to any of these drugs compared to wild type H99 (data not shown).

*kre5*Δ and *kre6*Δ*skn1*Δ cells have enlarged capsules with altered architectures

The *C. neoformans* cell wall is associated with two prominent virulence factors; the exopolysaccharide capsule and melanin (Chang and Kwon-Chung, 1994; Casadevall *et al*., 2000). Alterations in cell wall composition have been shown to adversely affect their production or attachment (Baker *et al*., 2007; Reese *et al*., 2007; Reese and Doering, 2003). Therefore, we examined both capsule and melanin in the deletion strains. Interestingly, when grown under capsule-inducing conditions and stained with India ink, the *kre5*Δ and

*kre6*Δ*skn1*Δ cells had enlarged capsules compared with those of wild type cells. A minimum of 200 cells from each strain were examined and the average capsule radius of wild type cells was 2.28 μm while the average radii of *kre5*Δ and *kre6*Δ*skn1*Δ capsules were 4.49 μm and 4.24 μm, respectively. Furthermore, the mutant capsules had a fainter, more diffuse appearance with rough edges, in contrast to the smooth ring of wild type capsule (Fig. 7A). There were several instances where the capsular polysaccharides appeared to slough from the capsule perimeter (Fig. 7A, arrows). The capsules of the remaining deletion strains had an appearance indistinguishable from wild type capsules (data not shown).

The altered appearance of the *kre5*Δ and *kre6*Δ*skn1*Δ capsules may have been the result of increased penetration of the India ink particles into the capsule interior, possibly due to alterations in capsular architecture. To test this idea, we measured the permeability of wild type and mutant capsules to TMR-dextrans of various sizes. The 70-kDa dextrans diffused further into the capsules of *kre5*Δ and *kre6*Δ*skn1*Δ cells than into wild type capsules, as indicated by a significant increase in the penetration zone (Fig. 7B). These data indicate that the capsules of the *kre5*Δ and *kre6*Δ*skn1*Δ mutants are more diffuse than the capsules of wild type cells.

Melanin production was assessed by growing strains on media containing the substrate L-DOPA (Polacheck *et al*., 1982; Williamson, 1994). All of the deletion strains produced a dark melanin pigment that remained associated with the cell, in contrast to the “leaky melanin” phenotype observed for other cell wall deficient mutants (Baker *et al*., 2007; Banks *et al*., 2005). However, both the *kre5*Δ and *kre6*Δ*skn1*Δ cells appeared slightly lighter in color compared to wild type cells (Fig. 8), indicating a possible decrease in total melanin production. As expected, a *lac1*Δ*lac2*Δ mutant (Missall *et al*., 2005) missing the enzymes responsible for melanin production produced no pigment.

Virulence analysis—The single deletion mutants were initially screened for alterations in virulence using STM analysis in a mouse tail vein model of infection (Nelson *et al*., 2001). Results from these preliminary experiments indicated that only *kre5*Δ and *kre6*Δ had consistent differences in virulence compared to wild type H99 (data not shown). Since these were also the only two single mutants to demonstrate altered phenotypes *in vitro* we analyzed them independently using a mouse inhalation model of infection. The *kre6*Δ*skn1*Δ double mutant and *kre6*Δ::*KRE6* complemented strain were also tested. We hypothesized that *kre5*Δ and *kre6*Δ*skn1*Δ would have decreased ability to cause mammalian infection, especially due to their inability to grow at 37°C. As anticipated, *kre5*Δ and *kre6*Δ*skn1*Δ were completely avirulent (Fig. 9). The *kre6*Δ mutant was also avirulent and this phenotype was rescued by reconstitution of the wild type gene. This result is somewhat surprising, as this mutant has wild type levels of β-1,6-glucan and displayed only a moderate sensitivity to SDS (Fig. 6B).

Cellular distribution of Phospholipase B1 is altered in kre5Δ and kre6Δskn1Δ

Plb1 is present in the cryptococcal cell wall and this localization requires the presence of its GPI-anchor (Djordjevic *et al*.,2005; Siafakas *et al*., 2006, Siafakas *et al*., 2007). Secreted Plb1 contains β-1,6-glucan (Siafakas *et al*., 2007). These data indicate that the cell wall is a source of Plb1 and that β-1,6-glucan is important for its attachment via a remnant of its GPI-anchor. To further explore this possibility, we next investigated whether reduced β-1,6-glucan in the *kre5*Δ and *kre6*Δ*skn1*Δ mutants coincided with altered Plb1 localization. Plb1 is a multifunctional enzyme displaying three activities (phospholipase B: PLB; lysophospholipase: LPL and lysophospholipase acyltransferase :LPTA). Almost all of the cell-associated and secreted PLB activity in *Cryptococcus* is attributable to the Plb1 protein (Cox *et al*. 2001; Wright *et al*. 2007), whereas the LPL and LPTA activities could also be

contributed by other enzymes (Coe *et al*. 2003; Wright *et al*. 2004). Therefore, we focused on the PLB activity.

Subcellular fractions were prepared from concentrated cryptococcal cell suspensions that had been allowed to secrete Plb1 overnight. The cell wall, ccrude membranes, cytosol and secretions were assayed for PLB activity using a radiometric enzyme assay. Overall, the mutants produced 2–3 times more total PLB activity (secreted and cell-associated) than the wild type (1705, 6348 and 4209 units for H99, *kre5*Δ and *kre6*Δ*skn1*Δ, respectively). Therefore, we compared PLB activity in corresponding fractions of wild type and each mutant strain by expressing the activity in each fraction as a percentage of the total activity in that strain (Fig. 10A). The percentage of cell wall-associated PLB activity was reduced in both the *kre5*Δ and *kre6*Δ*skn1*Δ mutants, with the reduction being greatest in *kre5*Δ (H99 183 units; *kre5*Δ, 1792 units; *kre6*Δ*skn1*Δ, 1734 units). This reduction in activity correlated with reduced retention of Plb1 protein in the cell wall fraction, as detected by Plb1 western blotting (Fig. 10B). The ratio of cell wall-associated/secreted PLB activity was 12, 0.72 and 1.6 for wild type, *kre5*Δ and *kre6*Δ*skn1*Δ, respectively, in this experiment, and 7.88, 0.88 and 2.35 in a second independent experiment. For each strain, PLB activity associated with the crude membrane fraction was negligible (H993; *kre5*Δ, 2; *kre6*Δ*skn1*Δ, 2 units). In strains with reduced cell wall-associated PLB activity, secretion of PLB activity (H99, 91 units; *kre5*Δ, 2474 units; *kre6*Δ*skn1*Δ, 1109 units) and Plb1 protein was concomitantly increased (Fig. 10A and 10B, respectively). Interestingly, Plb1 protein secreted by *kre5*Δ exhibited extensive breakdown (Fig. 10B, bottom arrow) despite the presence of protease inhibitors during sample preparation for SDS PAGE.

kre5Δ and kre6Δskn1Δ have altered chitosan staining but normal chitin and chitosan levels

Chitosan is an abundant polysaccharide in the vegetative cell wall of *C. neoformans*, and is important for maintaining cell wall integrity (Baker *et al*., 2007; Banks *et al*., 2005). Chitosan is produced by the removal of acetyl groups from nascent chitin polymers by chitin deacetylase (Cda) enzymes. The Cdas contain a putative GPI-anchor attachment motif (Baker *et al*., 2007) and have been identified in the extracellular proteome of *C. neoformans*, indicative of cell wall localization (Eigenheer *et al*., 2007). The loss of β-1,6-glucan in *kre5*Δ and *kre6*Δ*skn1*Δ may result in mis-localization or secretion of the cell wall associated Cdas, as was seen for Plb1. Such altered Cda localization could potentially result in reduced or altered cell wall chitosan. Therefore, we assessed cell wall chitosan by staining strains with the polyanionic dye eosin Y, which binds specifically to the positively charged chitosan in the *C. neoformans* cell wall under mildly acidic conditions (Baker *et al*., 2007). The *kre5*Δ and *kre6*Δ*skn1*Δ strains did not stain with eosin Y after 72 hours of growth (Fig. 11). This alteration in staining was specific for chitosan and not the result of a general cell wall defect, as pontamine staining produced the characteristic bright ring appearance (Fig. 5). The eosin Y staining patterns of the remaining single deletion strains were indistinguishable from that of wild type cells (data not shown). It has previously been shown that *chs3*Δ and *cda1*Δ*cda2*Δ*cda3*Δ mutants, which lack cell wall chitosan, do not stain with eosin Y (Baker *et al*., 2007). The loss of eosin Y staining observed for *kre5*Δ and *kre6*Δ*skn1*Δ suggested that levels of chitosan may be reduced. However, there was surprisingly no significant difference in the levels of either chitin or chitosan between wild type and *kre5*Δ or *kre6*Δ*skn1*Δ when measured biochemically (data not shown). Chitin/chitosan content of the remaining single deletion strains also did not deviate significantly from wild type levels (data not shown). We tested whether the apparent disparity between the eosin Y staining and biochemical measurement data could be due to differing phases of growth between wild type and the slow-growing mutant strains, as chitosan content increases during vegetative growth. In addition, the interaction between eosin Y and chitosan (pKa 6.3) is highly dependent

upon charge and a decrease in staining could be caused by changes in the cell wall microenvironment that decrease the binding efficiency between eosin Y and chitosan. Both of these possibilities are unlikely, as both *kre5*Δ and *kre6*Δ*skn1*Δ cultures reached stationary phase by 24 h and staining at both pH 5.0 and pH 6.0 did not result in eosin Y binding to the mutants (data not shown). Together these data indicate that the cell wall organization of *kre5*Δ and *kre6*Δ*skn1*Δ may be altered in such a way that chitosan is no longer accessible for binding by eosin Y.

DISCUSSION

The fungal cell wall is an ideal drug target, as it is essential for viability and absent from mammalian cells. The polysaccharide β-1,6-glucan is the most abundant β-glucan in the cell wall of the opportunistic pathogen *C. neoformans*. This work is the first report of the function of this polymer in *Cryptococcus*. We demonstrated that β-1,6-glucan, and the genes involved in its synthesis, namely *KRE5, KRE6* and *SKN1*, are critical for maintaining growth, morphology and cell wall integrity in *C. neoformans*. Their disruption also results in striking alterations to cell wall chitosan and important virulence factors including the exopolysaccharide capsule, the GPI-anchor mannoprotein Plb1 as well as loss of virulence in a mammalian host. These data indicate that β-1,6-glucan, along with being abundant, has in important function in the maintenance of cell wall organization and integrity in *C. neoformans*.

We sought first to determine whether the *KRE* genes identified were involved in β-1,6-glucan synthesis in *C. neoformans*. The data from dot blot analyses using polyclonal anti-β-1,6-glucan antiserum clearly demonstrated that disruption of *KRE5* or *KRE6* and *SKN1* in combination resulted in obvious, qualitative decreases in the level of this cell wall polymer. Although these results are dramatic, the actual levels of β-1,6-glucan cannot be quantified by these means. An alternative method for analyzing β-1,6-glucan levels would be to digest the cell wall with recombinant β-1,6-glucanase and measure the amount of reducing sugars released. However, the results garnered through this approach may still not necessarily reflect the true composition of the cryptococcal wall. There are only a few β-1,6-glucanases from different organisms which have been cloned and/or purified (de la Cruz *et al*., 1995, Boisramé and Gaillardin, 2009), but their specificities or activities have not been completely characterized, especially in the context of a complex mixture of polysaccharides present in a cell wall extract. Knowledge of specificity is crucial because, following glucanase treatment, free sugar ends are measured, therefore monomers, dimers, trimers, etc. are all detected. The β-1,6-glucanase from *Trichoderma harzianum* described by de la Cruz *et al*. (1995), although effective on purified β-1,6-glucan, was ineffective on cell wall preparations from two different fungal species. Only one β-1,6-glucanase has been used to characterize *S. cerevisiae* and *C. albicans* walls, and it is becoming clearer from our work and others (Banks *et al*., 2005, Reese *et al*., 2003) that the cryptococcal wall is more complex (containing chitosan and α-glucan) and likely organized very differently than the ascomycete wall. Although it is clear that the cryptococcal wall contains higher levels of β-1,6-glucan (James *et al*., 1990) the molecular organization of this polymer and the linkages with other cell wall components have not been defined biochemically. A further complication is the presence of the adjacent capsular polysaccharide of *C. neoformans*, which interferes with cell wall analysis, requiring the use of an acapsular background strain (James *et al*., 1990, Reese *et al*. 2007) that may not truly reflect the composition of a wild type cell wall. Future investigations of the biochemical composition and organization of the cryptococcal cell wall will certainly prove to be informative, providing that interpretations carefully consider these caveats.

Expansion of the KRE6/SKN1 gene family in C. neoformans

An interesting feature of β-1,6-glucan synthesis in *Cryptococcus* and other basidiomycetes is the expansion of the *KRE6*/*SKN1* gene family to multiple members. There are several possible explanations for the retention of such apparent redundancy within the cryptococcal genome. One reason may be that these genes function under various growth conditions or during different stages of the life cycle, such as during mating. Consistent with this idea, microarray analysis of RNA isolated from a *C. neoformans* serotype D strain revealed differential expression of the *KRE6/SKN1* genes during different stages of mating (Christina Hull, personal communication). It remains to be determined whether this phenomenon holds true for serotype A. Another interesting aspect is the correlation between the expansion of the *KRE6/SKN1* genes with the predominance of β-1,6-glucan polymer over that of β-1,3-glucan in *C. neoformans*. To date, the identity of the β-1,6-glucan synthase enzyme has remained elusive. There is no direct biochemical evidence that any of the *KRE* genes encode the protein required for enzymatic catalysis of β-1,6-glucan. The localization of Kre5p to the ER and the fact that a *kre5/kre5* mutant of *C. albicans* contains residual levels of β-1,6-glucan make it an unlikely candidate. The absence of apparent *KRE1, KRE11* or *KRE9/KNH1* homologs in basidiomycetes known to have β-1,6-glucan, including *C. neoformans*, argues against these genes filling the role of the synthase. It is tempting to speculate that the increased number of *KRE6/SKN1* genes coupled with the high levels of β-1,6-glucan suggest that this family could encode the synthases. Consistent with this idea, Kitamura *et al*. (2009) recently reported the identification of Kre6p as the target of a β-1,6-glucan small molecule inhibitor. Although β-1,6-glucan is still found in a *S. cerevisiae kre6*Δ*skn1*Δ strain, this polymer is smaller and has an altered structure (Roemer *et al*., 1993). Conversely, the presence of a Kre6p-related gene in *Aspergillus fumigatus*, which lacks β-1,6-glucan in its cell wall, appears to be evidence contradictory to this idea (Aimanianda *et al*., 2009). However, a similar condition exists in *Schizosaccharomyces pombe* where a chitin synthase is present in the genome but little to no chitin was found in the cell wall (Sietsma and Wessels, 1990, Bush *et al*., 1974). Studies using the recently published radiometric assay for β-1,6-glucan synthesis (Aimanianda *et al*., 2009) make the prospect of identification of the synthase enzyme(s) optimistic.

Loss of β-1,6-glucan disrupts chitosan localization

Alterations in the level of one cell wall polysaccharide are often accompanied by compensatory changes in the levels of other cell wall components. In *S. cerevisiae*, decreases in β-glucan levels can lead to increased chitin deposition in the cell wall to maintain cell integrity (Popolo *et al*. 1997; Bulik *et al*. 2003; Lesage *et al*. 2005; Reese *et al*. 2007). The *C. neoformans* cell wall is distinct from that of *S. cerevisiae* in that it has significant levels of chitosan, the deacetylated derivative of chitin. Both *kre5*Δ and *kre6*Δ*skn1*Δ had markedly decreased staining intensity with the chitosan-specific dye eosin Y. However, the levels of both chitin and chitosan in *kre5*Δ and *kre6*Δ*skn1*Δ were not significantly different from that in wild type cells grown under the same conditions. One possible explanation for this disparity is that chitosan distribution in the cell wall is altered in such a way that it is “masked” from eosin Y binding. Three chitin deacetylases (Cdas) are responsible for the production of cell wall chitosan by the enzymatic deacetylation of nascent chitin polymers (Baker *et al*. 2007). The Cdas contain a predicted GPI-anchor attachment motif and were identified in the *C. neoformans* extracellular proteome (Eigenheer *et al*. 2007; Baker *et al*. 2007). We hypothesize that altered chitosan distribution in *kre5*Δ and *kre6*Δ*skn1*Δ could result from altered localization of the Cdas, as was observed for Plb1. If the Cdas are absent from the cell wall of *kre5*Δ and *kre6*Δ*skn1*Δ but remain in the plasma membrane, chitosan could still be produced, but would now be generated in the interior of the cell wall, hidden from eosin Y binding.

Cryptococcus has seven chitin synthase (Chs) genes, but Chs3 is primarily responsible for the production of the chitin from which chitosan is derived. An alternative explanation for the loss of eosin Y staining is that Chs3 localization may be altered in *kre5*Δ and *kre6*Δ*skn1*Δ, possibly trapped in the membrane-bound "chitosomes" which contain chitin synthase activity (reviewed in Bartnicki-Garcia, 2006). Chitosomes are proposed sites of chitin microfibril synthesis, but trafficking of these vesicles is not understood. It is also not known whether the Cdas co-localize to these structures. The potential existence of secretory pathway defects in *kre5*Δ and *kre6*Δ*skn1*Δ could affect trafficking of Chs3 via chitosomes and hence prevent the chitin that is deacetylated to chitosan from reaching the cell wall. Investigation of the localization and interaction of the Cdas and Chs3 in wild type cells compared to *kre5*Δ and *kre6*Δ*skn1*Δ will provide further insight into the mechanism of chitosan production in *C. neoformans*.

KRE genes are important for maintaining capsule architecture

We have shown that disruption of *KRE5* or *KRE6* and *SKN1* in combination affects the size and architecture of the exopolysaccharide capsule, a primary *C. neoformans* virulence factor. The capsules of the *kre5*Δ and *kre6*Δ*skn1*Δ cells are enlarged, appear diffuse and are more permeable to TMR-labeled dextrans than the capsules of wild type cells. There are several possible explanations for these data, which are not mutually exclusive. First, Yoneda and Doering (2006) demonstrated that the capsular polysaccharide building block, GXM, is synthesized in vesicles within the cell and secreted at the cell surface, where it is attached to the cell wall via an unknown mechanism. The appearance of enlarged intracellular vesicular structures within the *kre5*Δ and *kre6*Δ*skn1*Δ cells, and the proposed localization of *KRE5* to the endoplasmic reticulum (Meaden *et al*., 1990) and *KRE6* and *SKN1* to the Golgi (Roemer *et al*., 1994) indicates potential disruption of the secretory pathway. Such disruption could account for alterations in capsule formation. It has also been shown that cell wall α-1,3-glucan is required for capsule attachment to the *C. neoformans* cell surface, although it is unknown whether this interaction is direct (Reese and Doering, 2003). It is possible that the diffuse appearance of the *kre5*Δ and *kre6*Δ*skn1*Δ capsule could result from decreased levels or altered distribution of α-1,3-glucan throughout the cell wall. Another study has implicated β-1,4-*N*-acetylglucosamine (GlcNAc) oligomers, which include both chitin and chitosan in *C. neoformans*, in the association of capsule with the cell wall (Rodrigues *et al*. 2008). Furthermore, mutants with decreased cell wall chitosan, particularly *chs3*Δ and *cda1*Δ*cda2*Δ*cda3*Δ, have enlarged capsules. The apparent alteration in chitosan localization in both *kre5*Δ and *kre6*Δ*skn1*Δ, indicated by the loss of eosin Y staining, is consistent with the idea that chitosan may play an important role in attachment or assembly of the capsule.

Loss of β-1,6-glucan results in secretion of GPI-anchored cell wall proteins, including Plb1

Another important cryptococcal virulence factor is Plb1. Previous studies have demonstrated that Plb1 is GPI-anchored and localized both in the plasma membrane and covalently linked to β-1,6-glucan in the cell wall (Siafakas *et al*., 2006; Siafakas *et al*., 2007). In *S. cerevisiae*, the majority of cell wall proteins are attached to β-1,6-glucan via a remnant of their GPI-anchor (Kapteyn *et al*., 1996; Yin *et al*., 2005). We hypothesized that the loss of β-1,6-glucan in *kre5*Δ and *kre6*Δ*skn1*Δ would result in decreased Plb1 retention in the cell wall and increased Plb1 secretion. Our results demonstrate that *kre5*Δ and *kre6*Δ*skn1*Δ have decreased Plb1 protein and activity associated with the cell wall, with a concomitant increase in the secretion of PLB activity and Plb1 protein (Fig. 9). Some PLB activity was still released from mutant cell walls by treatment with β-1,3-glucanse. This enzyme is unlikely to have been non-covalently associated with the cell wall, as extensive washing with saline was performed prior to treatment with β-1,3-glucanse. More likely, it represents enzyme that is covalently-associated to a different cell wall polysaccharide as a compensatory mechanism for the absence of β-1,6-glucan. Such altered cross-linking of cell

wall mannoproteins to cell wall polysaccharides has been observed in mutant strains with aberrant cell walls in *S. cerevisiae* (Kapteyn *et al*., 1997). The low PLB activity in the crude membrane preparations is most likely due to the sequestration of the Plb1 protein within the raft portion of these membranes, which were found previously to create a suppressive environment for PLB activity (Siafakas *et al*., 2006).

In summary, we have identified three genes, *KRE5, KRE6* and *SKN1* involved in β-1,6-glucan synthesis in *C. neoformans*. Our data demonstrate an important role for these genes and β-1,6-glucan in cell wall integrity, capsular architecture, virulence and the retention of cell wall mannoproteins. They are also important for cell wall organization, particularly chitosan distribution. This is the first investigation of β-1,6-glucan in *C. neoformans*. These findings provide the framework for future investigations into cell wall protein attachment as well as the mechanism of chitosan production in this important fungal pathogen.

EXPERIMENTAL PROCEDURES

Strains and media

The *C. neoformans* serotype A clinical isolate H99 was used as the wild type strain. *C. neoformans* was grown on YPD (1% yeast, 2% bacto-peptone, 2% dextrose), with solid media containing 2% bacto-agar. Selective YPD contained 200 units ml^{-1} hygromycin (Calbiochem, San Diego), 100 mg ml^{-1} nourseothricin (Werner BioAgents, Jena-Cospeda, Germany) or 200 μg ml^{-1} gentamicin (G418) (Invitrogen, Carlsbad, CA).

Identification of β-1,6-glucan synthesis-related protein sequences

The sequences of the *S. cerevisiae* Kre5p, Kre6p, Skn1p, Kre1p, Kre9p, Kre11p and Knh1p were used as a query sequences in BLASTp searches of the predicted proteins from the *C. neoformans* H99 genome (http://www.broad.mit.edu/annotation/genome/cryptococcus_neoformans/MultiHome.html). Seven proteins with an E-value < $1E^{-6}$ were identified. These were used in a reciprocal BLASTp analysis of the *S. cerevisiae* predicted proteins. The proposed name of the predicted *C. neoformans* protein was based on the reciprocal BLASTp analysis as well as the clustering observed in the phylogenetic analysis. The suggested names for the *C. neoformans KRE6* genes are based on the level of similarity to the known *S. cerevisiae* genes. For example, CNAG_00897 is most similar to the the *S. cerevisiae SKN1* gene and thus was designated *SKN1* whereas the remaining *C. neoformans* genes had a higher level of similarity to the *S. cerevisiae KRE6* gene and thus are designated *KRE6, KRE61, KRE62, KRE63* and *KRE64*. It is accepted practice to append a number onto the gene name when multiple *C. neoformans* genes share the highest level of similarity to a single *S. cerevisiae* gene.

RNA extraction and poly (A) RNA purification

H99 was grown for 24 h at 30°C or 37°C in liquid YPD medium and total RNA isolated as described (Baker *et al*., 2007). All samples had an OD 260/280 ratio of 1.8–2.0. Poly(A) RNA was purified from the total RNA sample by using an oligo-Tex RNA purification kit (QIAGEN, Valencia, CA) following the manufacturer's specifications.

Northern hybridizations

Analysis of mRNA levels by Northern blot was performed as described (Baker *et al*., 2007). The procedure used was adapted from that of Sambrook and Russell (2001). All gene-specific DNA probes were generated using H99 cDNA as template. Probes were designed to span an intron, to ensure specificity for RNA, not genomic DNA. Primers 17 and 18 were

used to amplify the *KRE5* probe while the remaining probes were amplified with primers 13 and 14 (Table S1).

Generation of deletion strains

All constructs used to generate single deletion mutants were made using overlap PCR gene deletion technology (Davidson *et al*., 2002) and were biolistically transformed (Toffaletti *et al*., 1993; Hua *et al*., 2000) into *C. neoformans* H99 to generate single deletion strains as described (Baker *et al*., 2007). Primer sequences are listed in Table S2. Each deletion construct included a hygromycin resistance cassette (Hua *et al*., 2000) for selection. Transformants that grew on selective media were passaged 5x on YPD then screened for homologous recombination at both the 5' and 3' end using PCR (Nelson *et al*., 2003) and a single site of integration was confirmed by Southern blot analysis as described (Baker *et al*., 2007). Isolates recovered from separate transformation plates were considered independent and used when complementation could not be acheived. The *kre6*Δ*skn1*Δ and *kre6*Δ*kre61*Δ double deletion strains were generated by biolistic transformation of a *KRE6* deletion construct containing a nourseothricin cassette (McDade and Cox, 2001) into the *skn1*Δ or *kre61*Δ backgrounds, respectively.

Generation of complemented deletion strain

The *kre6*Δ deletion strain was reconstituted using a method described previously (Goins *et al*., 2006). A PCR product containing the wild-type *KRE6* coding region plus 1000 bp of the upstream and 500 bp of the downstream untranslated regions was amplified from H99 genomic DNA using primers KRE6-1 and KRE6-2 listed in Table S1. This linear fragment along with a second, unlinked PCR product containing the G418 resistance cassette, were was biolistically co-transformed into *kre6*Δ. The transformants were screened by PCR for the presence of *KRE6* at the wildtype locus and for the absence of the deletion cassette. The same method was utilized without success to attempt to reconstitue *kre5*Δ with *KRE5* and *kre6*Δ*skn1*Δ with *KRE6*.

Isolation of cell wall material

Alkali-soluble cell wall material was prepared from H99 and the deletion strains using a modification of the procedures described by Maneesri *et al*. (2005) and Page *et al*. (2003). Strains were grown in 25 ml YPD at 30°C overnight with shaking. Cells were pelleted by centrifugation (650 g for 10 min), washed with 5 ml sterile water and resuspended in 0.5–1.0 ml sterile water. Cells were added to 1 volume glass beads (425–600 micron) and then lysed using a mini bead beater. Samples were beaten five times for 30 sec at 5K rpm, with intermittent incubation on ice. Lysate was removed from beads and protein content determined using the QuickStart Bradford assay kit (BioRad) with BSA as a standard. Volumes of lysate containing 8 μg protein were alkali-extracted with 50 μL 1.5N NaOH (total volume 100 μL) at 75°C for 1h. Samples were centrifuged 5 min at 11 000 g and the supernatants containing alkali-soluble glucans were removed. The alkali-insoluble pellets were resuspended in 50 μL of 100 mM K_2PO_4 buffer, pH 6.0 containing 0.2 U chitinase from *Serratia marcescens* (C1650; Sigma) and incubated at 37°C for 72h.

Dot blot assay

Serial two-fold dilutions of alkali-soluble material or the alkali-insoluble, chitinase-digested material were spotted onto nitrocellulose membranes. Spots were allowed to dry completely, and then the membrane was blocked with 10 ml TBST (25 mM Tris-HCl, pH 8.1, 0.15 M NaCl, 0.1% Tween-20) containing 5% non-fat milk powder for 1h at room temperature. Membranes were washed 3x with TBS (25 mM Tris-HCl, pH 8.1, 0.15 M NaCl) and then probed with rabbit polyclonal anti-β-1,6-glucan antiserum (1:1000) overnight at 4°C.

Membranes were washed as before and incubated with HRP-conjugated goat anti-rabbit secondary antibody for 1h at room temperature. Secondary antibody was detected with ECL reagent and signal analyzed by autoradiography.

For competition analysis, H99 alkali-soluble cell wall material was spotted onto membrane, as described above. The primary rabbit polyclonal anti-β-1,6-glucan antiserum working solution was preincubated with 5 μg/ml purified pustulan from *Umbilicaria pustulata* (400507; CarboMer, Inc) laminarin from *Laminaria digitata* (61430; Fluka), or mannan from *Saccaromyces cerevisiae* (M7504; Sigma) for 30 min with shaking prior to probing the blot as described above.

Fluorescence microscopy

For assessing morphology, cells were streaked on YPD plates and grown on YPD agar plates for 2 days at 30 °C. A loop of cells was then were resuspended in 180 μl PBS, and 20 μl of a 1:1,000 dilution of pontamine in PBS solution (Fast Scarlet 4B; Bayer Corp.) was added. Incubation was carried out and incubated at room temperature in the dark for 10 min. For assessing cell wall chitosan, strains were grown in 25 ml of YPD broth at 30°C for 24, 48 and 72 hours with shaking. At each time pointthe given timepoints, 0.5 ml of each culture was pelleted by centrifugation and washed with 1 ml McIlvaine's buffer [0.2 M Na_2HPO_4 and 0.1 M citric acid pH 6.0]. Cells were then resuspended in 0.5 ml McIlvaine's buffer containing with 30 μl eosin Y (5 mg ml^{-1} stock; Sigma, St. Louis, MO), incubated at room temperature in the dark for 10 minutes and washed twice, as before. Cells were examined with an Olympus Vanox AHBT3 microscope at 1000× magnification. Excitation wavelengths were 488 nm and 548 nm for eosin Y and pontamine, respectively.

Cell wall inhibitor assays

Strains were grown in 2 ml of YPD broth overnight at 30°C with shaking and then diluted to 1×10^7 cells ml^{-1}. Tenfold serial dilutions were made and 5 μl of each were plated onto solid YPD agarmedium without and with the designated amounts of calcofluor white (Fluorescent Brightner 28, Sigma F-3543), caffeine (Sigma, C-0750), SDS (AnalaR Biochemical, BDH Chemicals, Poole, UK) NaCl, sorbitol and Congo red (Sigma, C-6767). Plates were incubated at 30°C or 37°C and photographed after 2 and 7 days.

Antifungal testing

Etest strips (AB Biodisk) containing a gradient of fluconazole, voriconazole or caspofungin were used. Strains were grown in YPD overnight at 30°C, diluted to an OD650 of 0.1 and streaked in triplicate on RPMI-1640 (Sigma, R6504) agar to create even lawns. Antifungal strips were placed on the center of each plate and incubated at 30°C for 72h. MIC values were determined from two independent experiments according to the manufacturer's instructions.

Analysis of capsule production and architecture

Strains were streaked on YPD plates and grown on YPD agar plates for 2 days at 30°C. Cells from these plates were subcultured onto DME plates [13.4 g l^{-1} Dulbecco's modified Eagle's medium, 25mM MOPS pH 7.0, 1.8% agar] and incubated for 3 days at 30°C with 5% CO_2 to induce capsule production. Cells were resuspended in a 1:4 India ink:H_2O solution to visualize the capsule and observed through an Olympus AHBT3 microscope at 1000× magnification. Capsule radii were measured from digital images using Olympus Microsuite 5 software.

Capsule permeability assays using tetramethyl-rhodamine (TMR) conjugated dextrans were performed as described by Gates *et al*. (2004). Cells were diluted to 8×10^6 cells mL^{-1} in

PBS and 25 μL of each suspension was added to an equal volume of 10 kDa, 40 kDa or 70 kDa TMR-dextran solution (2 mg mL^{-1} in PBS). Samples were incubated in the dark at room temperature for 60 min and then observed through an OlympusVanox AHB2 microscope at 1000× magnification. Digital images were captured with an Olympus FVII digital camera and processed and analyzed with Olympus Microsuite 5 software. Since the *kre5*Δ and *kre6*Δ*skn1*Δ cells and capsules were enlarged compared to wild type, we modified the analysis to determine the "penetration zone," which is a measure of how far the TMR-dextrans diffused into the capsule (see Fig, 7B). Aliquots of the starting cultures were stained with India ink to measure capsule radius. The radius of exclusion of each cell was determined by subtracting the diameter of the cell (measured on the bright field image) from the diameter of the exclusion zone (measured on the fluorescent image) and dividing by 2. The radius of penetration is defined as: average capsule radius (measured by India ink staining)/radius of exclusion.

Analysis of melanin production

Strains were grown and diluted as per for the cell wall inhibitor assays, plated on L-DOPA-containing agar plates medium (13 mM glycine, 15 mM glucose, 29.4 mM KH_2PO_4, 10mM $MgSO_4$*$7H_2O$, 3.0 μM thiamine, 5.0 μM D-biotin, 1.0 mM L-DOPA, 2% bacto-agar) and assayed for melanin production by noting the color of the cells that grew after 2–7 days at 30°C.

Pooled mutant STM virulence analysis

Virulence of the single deletion strains was analyzed by signature tagged mutagenesis using a mouse tail vein model of infection, as described previously (Nelson *et al*., 2001).

Inhalation mouse model

Cryptococcus neoformans strains were grown at 30°C with shaking for 2 nights in YPD broth. The cells were centrifuged, washed, and resuspended in endotoxin-free PBS. The cells were counted on a hemocytometer and diluted to 2×10^7 cells/ml. CBA/J female mice (Jackson Laboratories) were anesthetized and allowed to inhale 1×10^6 (50 μl) cells that were dripped into the nares. Mice were weighed before and during the course of infection and sacrificed by CO_2 asphyxiation once their body weight had decreased to 80% of the pre-infection body weight. At this point, the mice showed signs of being morbidly ill, including a ruffled coat, lethargy, a hunched posture, unstable gait, and loss of appetite.

Phospholipase B1 analysis

Cryptococcal secretions and subcellular fractions were prepared essentially as described (Siafakas *et al*., 2007) with minor modifications. Cryptococcal cells, grown as SAB agar lawns for 72 h, were harvested, washed with saline and resuspended in secretion buffer (10 mM Immidazole pH 5.0, 2% glucose) as a concentrated suspension (approximately 1 ml buffer : 5 ml packed cell volume). Incubation was carried out overnight at 30°C. Cells were pelleted by centrifugation and the secretions collected. Cell pellets were washed once with saline and once with MES-buffered saline (MBS; 25 mM MES, 150 mM NaCl, 2 mM EDTA [pH 6.5]) and frozen at −80°C. Following thawing on ice, pellets were resuspended in 5 ml of pre-chilled MBS containing 0.1% [vol/vol] Triton X-100 [TX100] and a fungal-specific protease inhibitor cocktail [Sigma P8215], to achieve a 1:1 (buffer: packed cell volume) suspension, and 1 ml aliquots of the suspension were transferred to prechilled, 2 ml screw-capped eppendorf tubes containing 1 ml of 0.5 mm zirconia/silica beads (Biospec Products, Inc 11079105z). Suspensions were homogenized using a MiniBeadbeater-8 cell disrupter (Daintree Scientific) for three cycles of 1 min, with alternating 1-min cooling periods on ice and the cell lysates were transferred to a fresh prechilled eppendorf tube. The

beads were washed with 0.5 ml MBS containing 0.1% Triton X-100 [TX100] and protease inhibitors, and the wash was combined with the lysate to maximise protein recovery. Cell lysates were centrifuged at 3,500 × g for 10 min at 4°C and the supernatants collected and set aside on ice. The 3,500 × *g* cell wall-containing pellets were washed three times with 30 ml saline and resuspended in 1.5–2.0 ml of β-1,3-glucanase lysing enzyme (Sigma L1412; 20 mg/ml made up in water and protease inhibitors). Incubation was carried out for 1 h with agitation at 37°C and the supernatant, containing released Plb1 and defined as the cell wall-fraction, was collected by centrifugation (14,000 × g for 15 min at 4°C). The 3,500 × *g* supernatants were centrifuged at 135,000 × g (45,000 rpm) for 1 h at 4°C in a Beckman bench-top ultracentrifuge fitted with a TLA45 rotor, to separate the pellet (crude membranes) and the supernatant (cytosol). Crude membranes were resuspended in 200 µl of ice-cold MBS containing protease inhibitors, probe sonicated for 3 to 4 s to create a suspension. Five µl of (G)PIPLC (*B. cereus*, 0.5–1 Units) was added to release GPI anchored proteins by incubation at 37°C for 1 h. The released GPI anchored proteins including Plb1 (supernatant), were collected by ultracentrifugation and are representative of the membrane-associated Plb1 fraction (Siafakas *et al*., 2007). The Plb1 content of all fractions was analyzed by western blotting with anti Plb1 peptide antibodies or by radiometric enzyme assay, where 1 unit=amount of enzyme hydrolyzing 1 nmol substrate per min, as previously described (Chen *et al*., 1997).

Cellular chitin and chitosan content assays

The chitin and chitosan content of cells was measured as described previously (Baker *et al*., 2007). Samples were divided into two aliquots. One aliquot was treated with acetic anhydride to measure chitin plus chitosan, and the second aliquot remained untreated to measure chitin. The difference between the two measurements was an estimate of the amount of chitosan.

Supplementary Material

Refer to Web version on PubMed Central for supplementary material.

Acknowledgments

We would like to thank Piet de Groot for supplying the polyclonal anti-β-1,6-glucan antiserum and Christina Hull for communication regarding serotype D microarrays. We also thank Leona Campbell and Woei Lam for helpful suggestions. This work was supported by National Institute of Health grants RO1AI072195 and RO1AI50184 to JKL and an American Heart Association predoctoral fellowship to NMG.

REFERENCES

Aimanianda V, Clavaud C, Simenel C, Fontaine T, Delepierre M, Latge JP. Cell Wall {beta}-(1,6)-Glucan of Saccharomyces cerevisiae: Structural characterization and *in situ* synthesis. J Biol Chem. 2009; 284:13401–13412. [PubMed: 19279004]

Araki Y, Ito E. A pathway of chitosan formation in *Mucor rouxii*. Enzymatic deacetylation of chitin. Eur J Biochem. 1975; 55:71–78. [PubMed: 240696]

Baker LG, Specht CA, Donlin MJ, Lodge JK. Chitosan, the deacetylated form of chitin, is necessary for cell wall integrity in *Cryptococcus neoformans*. Eukaryot Cell. 2007; 6:855–867. [PubMed: 17400891]

Banks IR, Specht CA, Donlin MJ, Gerik KJ, Levitz SM, Lodge JK. A chitin synthase and its regulator protein are critical for chitosan production and growth of the fungal pathogen *Cryptococcus neoformans*. Eukaryot Cell. 2005; 4:1902–1912. [PubMed: 16278457]

Bartnicki-Garcia S. Chitosomes: past, present and future. FEMS Yeast Res. 2006; 6:957–965. [PubMed: 16981903]

Boisramé A, Gaillardin C. Heterologous expression and characterization of a beta-1,6-glucanase from *Aspergillus fumigatus*. Appl Microbiol Biotechnol. 2009; 82:663–669. [PubMed: 19039584]

Bulik DA, Olczak M, Lucero HA, Osmond BC, Robbins PW, Specht CA. Chitin synthesis in *Saccharomyces cerevisiae* in response to supplementation of growth medium with glucosamine and cell wall stress. Eukaryot Cell. 2003; 2:886–900. [PubMed: 14555471]

Bush DA, Horisberger M, Horman I, Wursch P. The Wall Structure of *Schizosaccharomyces pombe*. J Gen Microbiol. 1974; 81:199–206. [PubMed: 4822119]

Casadevall A, Rosas AL, Nosanchuk JD. Melanin and virulence in *Cryptococcus neoformans*. Curr Opin Microbiol. 2000; 3:354–358. [PubMed: 10972493]

Chang YC, Kwon-Chung KJ. Complementation of a capsule-deficient mutation of *Cryptococcus neoformans* restores its virulence. Mol Cell Biol. 1994; 14:4912–4919. [PubMed: 8007987]

Chen SC, Muller M, Zhou JZ, Wright LC, Sorrell TC. Phospholipase activity in *Cryptococcus neoformans*: a new virulence factor? J Infec Dis. 1997; 175:414–420. [PubMed: 9203663]

Coe JGS, Wilson CF, Sorrell TC, Latouche NG, Wright LC. Cloning of CnLYSO1, a novel extracellular lysophospholipase of the pathogenic fungus *Cryptococcus neoformans*. Gene. 2003; 316:67–78. [PubMed: 14563553]

Cox GM, McDade HC, Chen SC, Tucker SC, Gottfredsson M, Wright LC, Sorrell TC, et al. Extracellular phospholipase activity is a virulence factor for *Cryptococcus neoformans*. Mol Microbiol. 2001; 39:166–175. [PubMed: 11123698]

de la Cruz J, Pintor-Toro JA, Benitez T, Llobell A. Purification and characterization of an endo-beta-1,6-glucanase from Trichoderma harzianum that is related to its mycoparasitism. J. Bacteriol. 1995; 177:1864–1871. [PubMed: 7896713]

Davidson RC, Blankenship JR, Kraus PR, de Jesus Berrios M, Hull CM, D'Souza C, Wang P, Heitman J. A PCR-based strategy to generate integrative targeting alleles with large regions of homology. Microbiology (Reading, Engl). 2002; 148:2607–2615.

Djordjevic JT, Del Poeta M, Sorrell TC, Turner KM, Wright LC. Secretion of cryptococcal phospholipase B1 (PLB1) is regulated by a glycosylphosphatidylinositol (GPI) anchor. Biochem J. 2005; 389:803–812. [PubMed: 15826239]

Eigenheer RA, Lee YJ, Blumwald E, Phinney BS, Gelli A. Extracellular glycosylphosphatidylinositol-anchored mannoproteins and proteases of *Cryptococcus neoformans*. FEMS Yeast Res. 2007; 7:499–510. [PubMed: 17233760]

Gates MA, Thorkildson P, Kozel TR. Molecular architecture of the *Cryptococcus neoformans* capsule. Mol Microbiol. 2004; 52:13–24. [PubMed: 15049807]

Goins CL, Gerik KJ, Lodge JK. Improvements to gene deletion in the fungal pathogen *Cryptococcus neoformans*: absence of Ku proteins increases homologous recombination, and co-transformation of independent DNA molecules allows rapid complementation of deletion phenotypes. Fungal Genet Biol. 2006; 43:531–544. [PubMed: 16714127]

de Groot PWJ, Yin QY, Weig M, Sosinska GJ, Klis FM, de Koster CG. Mass spectrometric identification of covalently bound cell wall proteins from the fission yeast *Schizosaccharomyces pombe*. Yeast. 2007; 24:267–278. [PubMed: 17230583]

Hartland RP, Vermeulen CA, Klis FM, Sietsma JH, Wessels JG. The linkage of (1–3)-beta-glucan to chitin during cell wall assembly in *Saccharomyces cerevisiae*. Yeast. 1994; 10:1591–1599. [PubMed: 7725794]

Herrero AB, Magnelli P, Mansour MK, Levitz SM, Bussey H, Abeijon C. *KRE5* gene null mutant strains of *Candida albicans* are avirulent and have altered cell wall composition and hypha formation properties. Eukaryot Cell. 2004; 3:1423–1432. [PubMed: 15590817]

Hoch HC, Galvani CD, Szarowski DH, Turner JN. Two new fluorescent dye applicable for visualization of fungal cell walls. *Mycologia*. 2005; 97(no. 3):580–588. [PubMed: 16392246]

Hochstenbach F, Klis FM, van den Ende H, van Donselaar E, Peters PJ, Klausner RD. Identification of a putative alpha-glucan synthase essential for cell wall construction and morphogenesis in fission yeast. Proc Nat Acad Sci USA. 1998; 95:9161–9166. [PubMed: 9689051]

Hua J, Meyer JD, Lodge JK. Development of positive selectable markers for the fungal pathogen *Cryptococcus neoformans*. Clin Diagn Lab Immunol. 2000; 7:125–128. [PubMed: 10618292]

James PG, Cherniak R, Jones RG, Stortz CA, Reiss E. Cell-wall glucans of *Cryptococcus neoformans* Cap 67. Carbohydr Res. 1990; 198:23–38. [PubMed: 2191777]

Kapteyn JC, Montijn RC, Vink E, de la Cruz J, Llobell A, Douwes JE, et al. Retention of *Saccharomyces cerevisiae* cell wall proteins through a phosphodiesterlinked beta-1,3-/beta-1,6-glucan heteropolymer. Glycobiology. 1996; 6:337–345. [PubMed: 8724141]

Kapteyn JC, Ram AF, Groos EM, Kollar R, Montijn RC, Van Den Ende H, et al. Altered extent of cross-linking of beta1,6-glucosylated mannoproteins to chitin in *Saccharomyces cerevisiae* mutants with reduced cell wall beta1,3-glucan content. JBacteriol. 1997; 179:6279–6284. [PubMed: 9335273]

Kitamura A, Someya K, Hata M, Nakajima R, Takemura M. Discovery of a Small-Molecule Inhibitor of β-1,6-Glucan Synthesis. Antimicrob Agen Chemo. 2009; 53:670–677.

Klis FM, De Groot P, Hellingwerf K. Molecular organization of the cell wall of *Candida albicans*. Med Mycol. 2001; 39 Suppl 1:1–8. [PubMed: 11800263]

Klis FM, Boorsma A, De Groot PW. Cell wall construction in *Saccharomyces cerevisiae*. Yeast. 2006; 23:185–202. [PubMed: 16498706]

Lesage G, Shapiro J, Specht CA, Sdicu A, Ménard P, Hussein S, et al. An interactional network of genes involved in chitin synthesis in *Saccharomyces cerevisiae*. BMC Genet. 2005; 6:8. [PubMed: 15715908]

Levitz SM, Specht CA. The molecular basis for the immunogenicity of *Cryptococcus neoformans* mannoproteins. FEMS Yeast Res. 2006; 6:513–524. [PubMed: 16696647]

López-Sáez JF, Mingo R, González-Fernández A. ATP level and caffeine efficiency on cytokinesis inhibition in plants. Eur J Cell Biol. 1982; 27:185–190. [PubMed: 7117265]

Maneesri J, Azuma M, Sakai Y, Igarashi K, Matsumoto T, Fukuda H, et al. Deletion of *MCD 4* involved in glycosylphosphatidylinositol (GPI) anchor synthesis leads to an increase in beta-1,6-glucan level and a decrease in GPI-anchored protein and mannan levels in the cell wall of *Saccharomyces cerevisiae*. J Biosci Bioeng. 2005; 99:354–360. [PubMed: 16233801]

McDade HC, Cox GM. A new dominant selectable marker for use in *Cryptococcus neoformans*. Med Mycol. 2001; 39:151–154. [PubMed: 11270405]

Meaden P, Hill K, Wagne rJ, Slipetz D, Sommer SS, Bussey H. The yeast *KRE5* gene encodes a probable endoplasmic reticulum protein required for (1----6)-beta- D-glucan synthesis and normal cell growth. Mol Cell Biol. 1990; 10:3013–3019. [PubMed: 2188106]

Missal TA, Moran JM, Corbett JA, Lodge JK. Distinct stress responses of two functional laccases in *Cryptococcus neoformans* are revealed in the absence of the thiol-specific antioxidant Tsa1. Eukaryot Cell. 2005; 4:202–208. [PubMed: 15643075]

Nelson RT, Huaa J, Pryor BA, Lodge JK. Identification of Virulence Mutants of the Fungal Pathogen *Cryptococcus neoformans* Using Signature-Tagged Mutagenesis. Genetics. 2001; 157:935–947. [PubMed: 11238384]

Nelson RT, Pryor BA, Lodge JK. Sequence length required for homologous recombination in *Cryptococcus neoformans*. Fungal Genet Bio. 2003; 38:1–9. [PubMed: 12553931]

Pagé N, Gérard-Vincent M, Ménard P, Beaulieu M, Azuma M, Dijkgraaf GJP, et al. A *Saccharomyces cerevisiae* genome-wide mutant screen for altered sensitivity to K1 killer toxin. Genetics. 2003; 163:875–894. [PubMed: 12663529]

Polacheck I, Hearing VJ, Kwon-Chung KJ. Biochemical studies of phenoloxidase and utilization of catecholamines in *Cryptococcus neoformans*. J Bacteriol. 1982; 150:1212–1220. [PubMed: 6804439]

Popolo L, Gilardelli D, Bonfante P, Vai M. Increase in chitin as an essential response to defects in assembly of cell wall polymers in the *ggp1*delta mutant of *Saccharomyces cerevisiae*. Bacteriol. 1997; 179:463–469.

Reese AJ, Doering TL. Cell wall alpha-1,3-glucan is required to anchor the *Cryptococcus neoformans* capsule. Mol Microbiol. 2003; 50:1401–1409. [PubMed: 14622425]

Reese AJ, Yoneda A, Breger JA, Beauvais A, Liu H, Griffith CL, et al. Loss of cell wall alpha(1–3) glucan affects *Cryptococcus neoformans* from ultrastructure to virulence. Mol Microbiol. 2007; 63:1385–1398. [PubMed: 17244196]

Rodrigues ML, Alvarez M, Fonseca FL, Casadevall A. Binding of the wheat germ lectin to *Cryptococcus neoformans* suggests an association of chitinlike structures with yeast budding and capsular glucuronoxylomannan. Eukaryot Cell. 2008; 7:602–609. [PubMed: 18039942]

Roemer T, Bussey H. Yeast beta-glucan synthesis: *KRE6* encodes a predicted type II membrane protein required for glucan synthesis *in vivo* and for glucan synthase activity *in vitro*. Proc Natl Acad Sci U.S.A. 1991; 88:11295–11299. [PubMed: 1837148]

Roemer T, Delaney S, Bussey H. *SKN1* and *KRE6* define a pair of functional homologs encoding putative membrane proteins involved in beta-glucan synthesis. Mol Cell Biol. 1993; 13:4039–4048. [PubMed: 8321211]

Roemer T, Paravicini G, Payton MA, Bussey H. Characterization of the yeast (1-->6)-beta-glucan biosynthetic components, Kre6p and Skn1p, and genetic interactions between the *PKC1* pathway and extracellular matrix assembly. J Cell Biol. 1994; 127:567–579. [PubMed: 7929594]

Roncero C, Durán A. Effect of Calcofluor white and Congo red on fungal cell wall morphogenesis: *in vivo* activation of chitin polymerization. J Bacteriol. 1985; 163:1180–1185. [PubMed: 3897187]

Ruiz-Herreraa J, Ortiz-Castellanosa L, Martínezb AI, León-Ramíreza C, Sentandreub R. Analysis of the proteins involved in the structure and synthesis of the cell wall of *Ustilago maydis*. Fungal Genet Biol. 2008; 45:S71–S76. [PubMed: 18508396]

Sambrook, J.; Russell, D. Molecular cloning: a laboratory manual. 3rd ed. Cold Spring Harbor, N.Y.: Cold Spring Harbor Laboratory Press; 2001.

Shahinian S, Bussey H. beta-1,6-Glucan synthesis in *Saccharomyces cerevisiae*. Mol Microbiol. 2000; 35:477–489. [PubMed: 10672173]

Shaw JA, Mol PC, Bowers B, Silverman SJ, Valdivieso MH, Durán A, et al. The function of chitin synthases 2 and 3 in the *Saccharomyces cerevisiae* cell cycle. J Cell Biol. 1991; 114:111–123. [PubMed: 2050738]

Shematek EM, Braatz JA, Cabib E. Biosynthesis of the yeast cell wall. I. Preparation and properties of beta-(1 leads to 3)glucan synthetase. J Biol Chem. 1980; 255:888–894. [PubMed: 6766139]

Siafakas AR, Sorrell TC, Wright LC, Wilson C, Larsen M, Boadle R, et al. Cell wall-linked cryptococcal phospholipase B1 is a source of secreted enzyme and a determinant of cell wall integrity. J Biol Chem. 2007; 282:37508–37514. [PubMed: 17947228]

Siafakas AR, Wright LC, Sorrell TC, Djordjevic JT. Lipid rafts in *Cryptococcus neoformans* concentrate the virulence determinants phospholipase B1 and Cu/Zn superoxide dismutase. Eukaryot Cell. 2006; 5:488–498. [PubMed: 16524904]

Sietsma JH, Wessels JG. The occurrence of glucosaminoglycan in the wall of *Schizosaccharomyces pombe*. J Gen Microbiol. 1990; 136:2261–2265. [PubMed: 2079623]

Toffaletti DL, Rude TH, Johnston SA, Durack DT, Perfect JR. Gene transfer in *Cryptococcus neoformans* by use of biolistic delivery of DNA. J Bacteriol. 1993; 175:1405–1411. [PubMed: 8444802]

Williamson PR. Biochemical and molecular characterization of the diphenol oxidase of *Cryptococcus neoformans*: identification as a laccase. J of Bacteriol. 1994; 176:656–664. [PubMed: 8300520]

Wright LC, Payne J, Santangelo RT, Simpanya MF, Chen SCA, Widmer F, et al. Cryptococcal phospholipases: a novel lysophospholipase discovered in the pathogenic fungus *Cryptococcus gattii*. Biochem J. 2004; 384:377–384. [PubMed: 15320865]

Wright LC, Santangelo RM, Ganendren R, Payne J, Djordjevic JT, Sorrell TC. Cryptococcal lipid metabolism: phospholipase B1 is implicated in transcellular metabolism of macrophage-derived lipids. Eukaryot Cell. 2007; 6:37–47. [PubMed: 17099081]

Yin QY, de Groot PWJ, Dekker HL, de Jong L, Klis FM, de Koster CG. Comprehensive proteomic analysis of *Saccharomyces cerevisiae* cell walls: identification of proteins covalently attached via glycosylphosphatidylinositol remnants or mild alkalisensitive linkages. J Biol Chem. 2005; 280:20894–20901. [PubMed: 15781460]

Yoneda A, Doering TL. A eukaryotic capsular polysaccharide is synthesized intracellularly and secreted via exocytosis. Mol Biol Cell. 2006; 17:5131–5140. [PubMed: 17021252]

Ziman M, Chuang JS, Schekman RW. Chs1p and Chs3p, two proteins involved in chitin synthesis, populate a compartment of the *Saccharomyces cerevisiae* endocytic pathway. Mol Biol Cell. 1996; 7:1909–1919. [PubMed: 8970154]

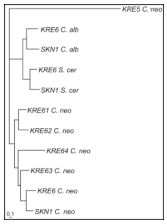

Fig. 1.

Phylogenetic tree of the Kre6/Skn1 proteins. The tree was created using the neighbor-joining algorithm in Phylip from a multiple alignment of the Kre6 and Skn1 protein sequences from *S. cerevisiae*, *C.neoformans*, and *C. albicans*, with the *C. neoformans* Kre5 protein used as an out group.

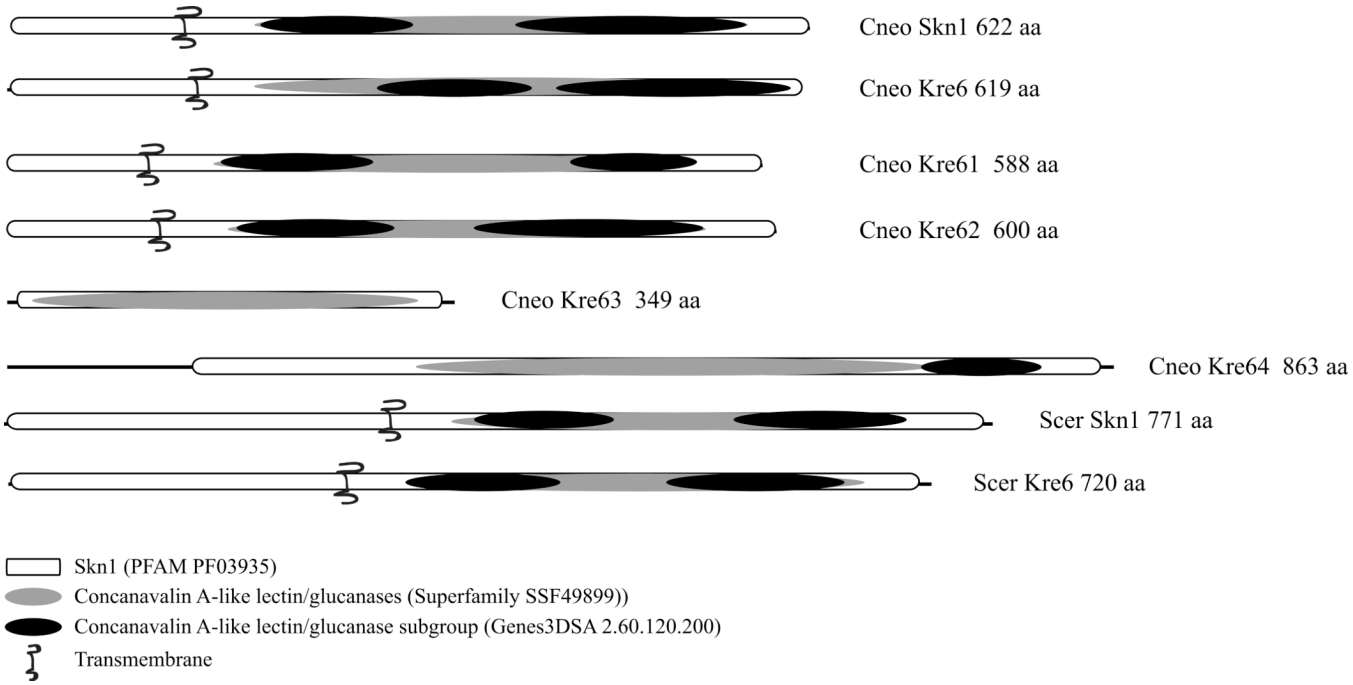

Fig. 2.

Domain organization of *C. neoformans* and *S. cerevisiae* Kre6/Skn1 homologs. Domains were identified using InterProScan.

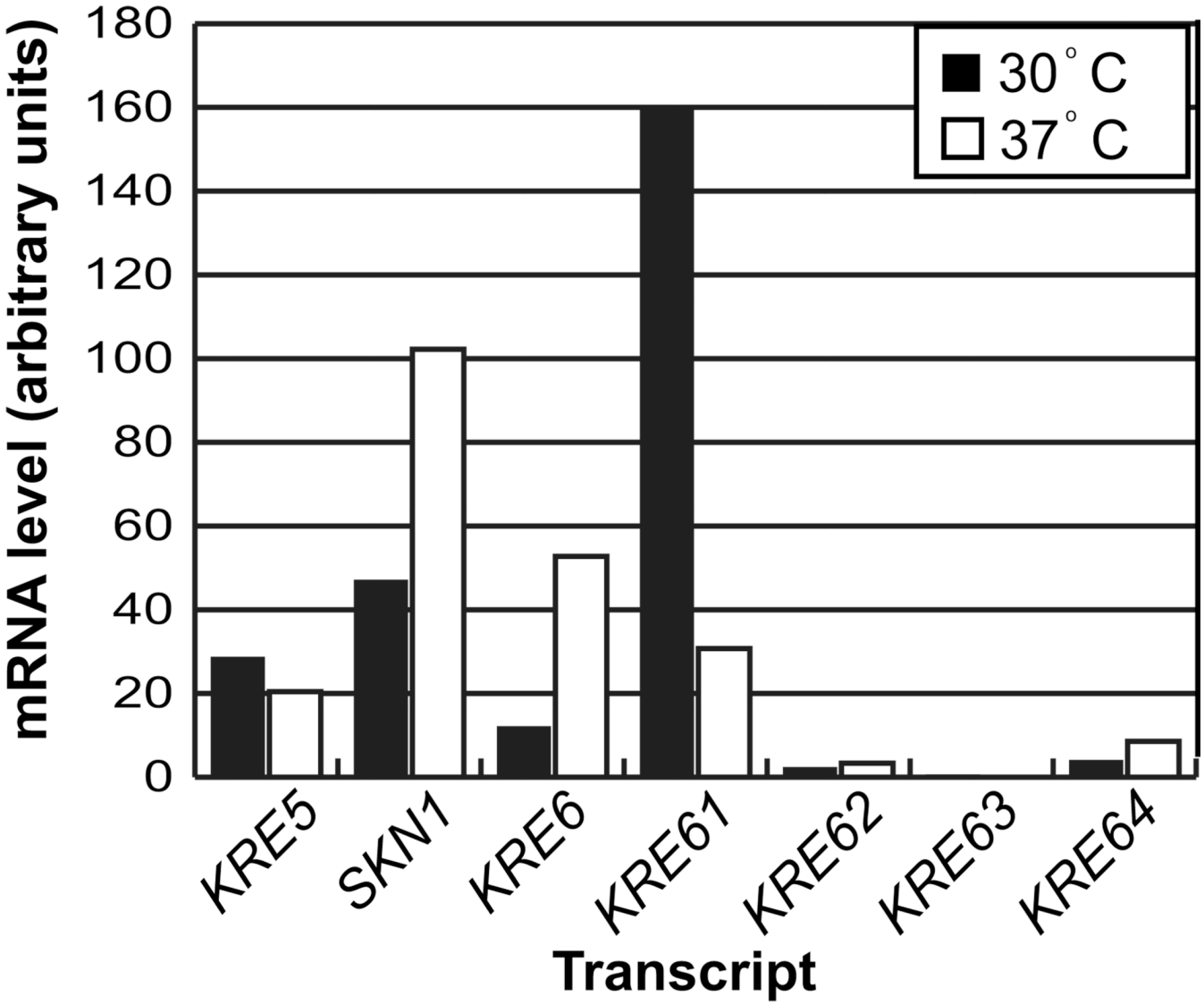

Fig. 3.

Northern blot mRNA expression analysis of *KRE5* and the *KRE6/SKN1* homologs in *C. neoformans*. H99 was grown in liquid culture for 24 h at the indicated temperatures. Relative gene expression was determined utilizing ImageQuant (version 5.1) and was normalized to the level of actin. Values are the average of two independent biological replicates.

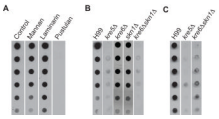

Fig. 4.

β-1,6-glucan dot blot assay. (A) Polysaccharide competition analysis. Alkali soluble cell wall material from H99 was spotted onto membrane. The primary anti-β-1,6-glucan antiserum was preincubated with the indicated purified polysaccharides for 30 min before probing the membrane. (B) Alkali-soluble cell wall β-1,6-glucan analysis of H99 and deletion strains. Cells were grown at 30°C to mid-log phase and alkali-soluble polysaccharides were isolated and spotted in 1:2 serial dilutions onto nitrocellulose membrane. Membranes were probed with polyclonal anti-β-1,6-glucan antiserum. (C) Alkali-insoluble, chitinase-released cell wall β-1,6-glucan analysis of H99 and deletion strains.

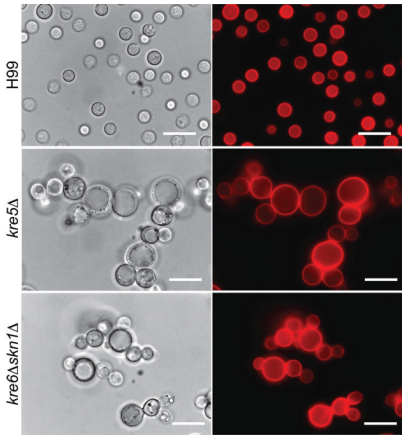

Fig. 5.

Morphology of *C. neoformans* H99, *kre5*Δ and *kre6*Δ*skn1*Δ. Cells were grown on YPD medium at 30°C for 72h and stained with Pontamine FastScarlet. All images are at 1000X magnification. Scale bar = 25μm.

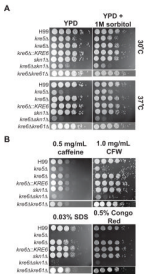

Fig. 6.

Sensitivity of mutants to temperature (A) and cell wall inhibitors (B). Strains were grown overnight in YPD medium, then diluted to an OD_{650} of 1.0. Tenfold serial dilutions were made in PBS and 5 µl of each was spotted on medium containing the indicated inhibitors. Plates were incubated at the indicated temperatures for 2 days.

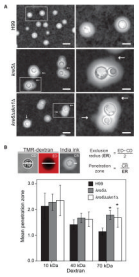

Fig. 7.

Capsule analysis (A) India ink staining of capsule of H99 and deletion strains. Strains grown for 3 days on DME medium at 30°C with 5% CO2 to induce capsule production were stained with India ink and visualized by light microscope. Arrows point to the rough appearance of the polysaccharide sloughing from capsular edge. Scale bars in the left and right panels are 25 and 10 μm, respectively. (B) Penetration of the cryptococcal capsule by TMR-dextrans. Top panel shows representative images of wild type cells stained with India ink or incubated with 70 kDa TMR-dextran and illustrates the measurements taken and the equations used to calculate the penetration zone. CD = capsule diameter; ED = exclusion diameter; CR = capsule radius. Strains were grown as in (A) and incubated 60 min with TMR-dextrans with average molecular masses of 10, 40 and 70 kDa, and the radius of penetration was determined by examination of digital images. Results shown are mean ± SD for at least 24 cells in two independent biological replicates. * denotes p≤ 0.02 compared to wild type H99 with 70 kDa dextran.

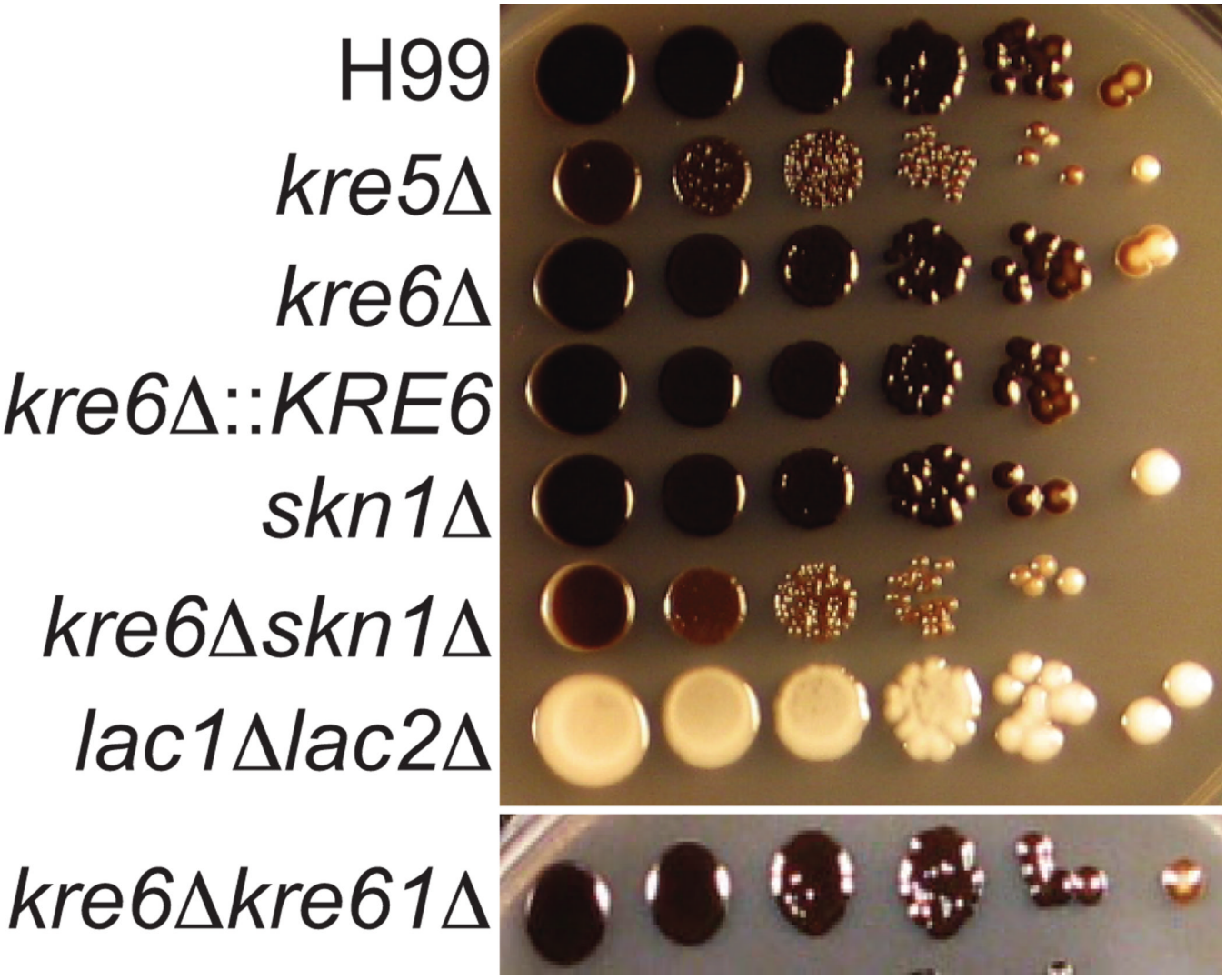

Fig. 8.

Melanin production. Strains were grown overnight in YPD medium, diluted to an OD_{650} of 1.0. and 5 μl of each tenfold serial dilution (in PBS) and was plated on medium containing 1 mM L-DOPA. Plates were incubated at 30°C for 7 days.

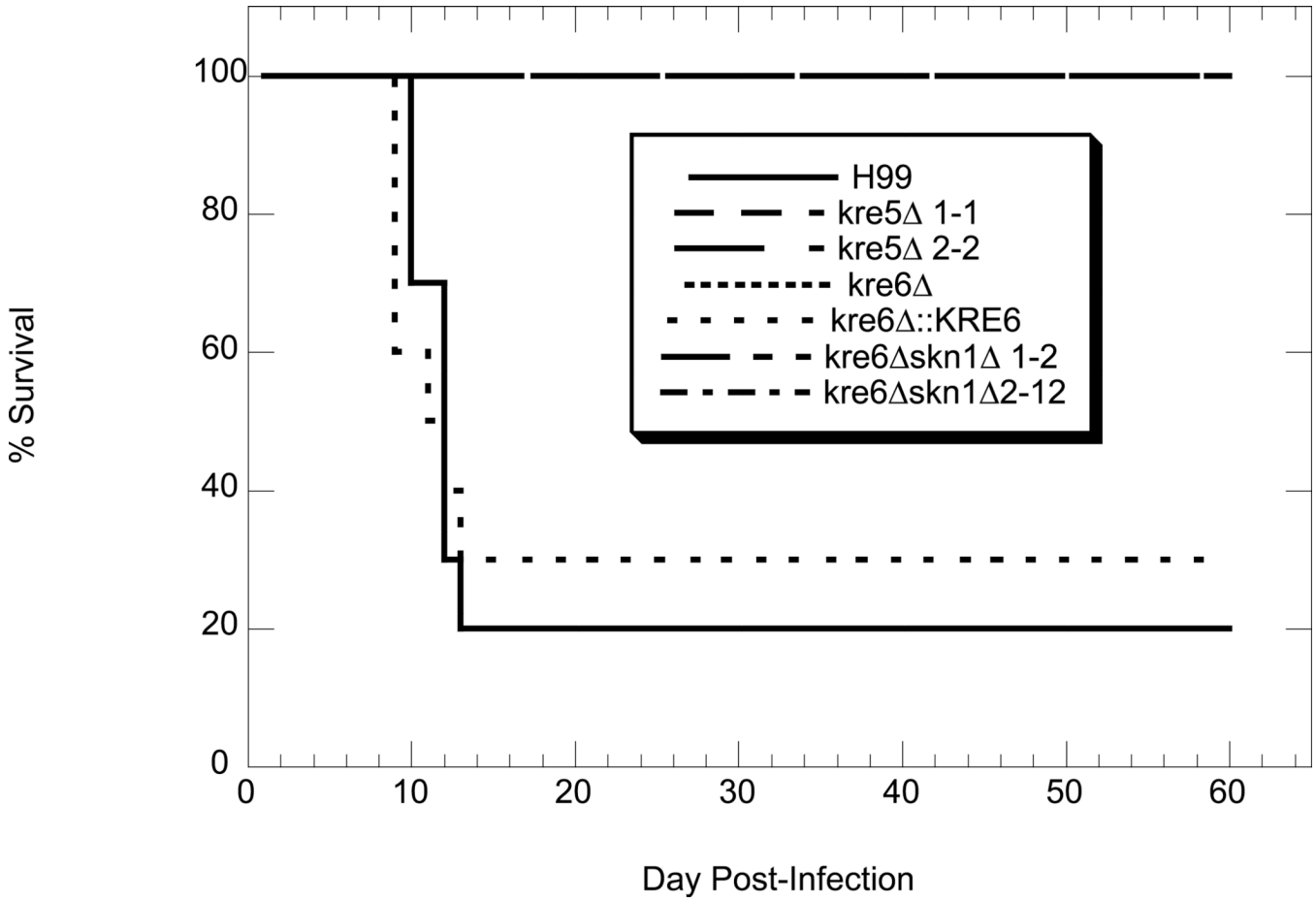

Fig. 9.

Virulence analysis. Mice (10 per strain) were inoculated with 1×10^6 cryptococcal cells, dripped into the nares. Mice were weighed before infection and sacrificed once they reached 80% of their original body weight.

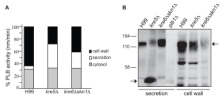

Fig. 10.

Cellular distribution of PLB activity (A) and the Plb1 protein (B). (A) Subcellular fractions were prepared from concentrated cell suspensions after an overnight incubation period and harvesting of the secreted proteins. PLB activity in the crude membrane fraction was negligible. * denotes $p<0.005$ (unpaired 2-tail t-test) compared to the corresponding fraction from H99. Similar results for all three strains were obtained in a second independent experiment (not shown). (B) Plb1 protein in the secreted and cell wall fractions were detected by western blotting with an anti-Plb1 peptide antibody. Top and bottom arrows indicate the position of full-length, fully glycosylated Plb1 and a breakdown product (most prominent in *kre5*Δ secretions), respectively.

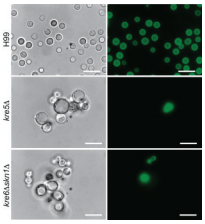

Fig. 11.

Eosin Y staining of H99 and *kre5*Δ and *kre6*Δ*skn1*Δ. Strains were incubated at 30 °C for 72 hours and stained with eosin Y. Images were captured at 1000X magnification. Bright cells in the eosin Y panels of the mutants are presumably dead cells that have taken up dye, as seen previously (Gerik *et al*. 2008). Scale bar = 25μm.

Table 1

Identification of *C. neoformans KRE5* and *KRE6/SKN1* genes

S.cerevisiae **Protein**	***C. neoformans*** **Broad Protein Match**	**BLASTp e-value**	***C. neoformans*** **Proposed Gene Name**
Kre5p	CNAG_03648.2	6.00E-24	*KRE5*
Skn1p	CNAG_00897.2	1.00E-114	*SKN1*
Kre6p	CNAG_00914.2	1.00E-113	*KRE6*
Kre6p	CNAG_06835.2	1.00E-116	*KRE61*
Kre6p	CNAG_06832.2	1.00E-109	*KRE62*
Kre6p	CNAG_06031.2	1.00E-73	*KRE63*
Kre6p	CNAG_05815.2	1.00E-90	*KRE64*

Table 2

Comparison of *S. cerevisiae* and *C. neoformans* Kre6/Skn1 proteins

Protein 1	Protein 2	% identity	% similarity
S. cerevisiae Kre6p	*C. neoformans* Kre6	45	62
S. cerevisiae Kre6p	*C. neoformans* Kre61	42	56
S. cerevisiae Kre6p	*C. neoformans* Kre62	46	61
S. cerevisiae Kre6p	*C. neoformans* Kre63	41	53
S. cerevisiae Kre6p	*C. neoformans* Kre64	38	53
S. cerevisiae Kre6p	*C. neoformans* Skn1	44	58
S. cerevisiae Skn1p	*C. neoformans* Skn1	48	61
S. cerevisiae Skn1p	*C. neoformans* Kre6	41	58
S. cerevisiae Kre6p	*C. albicans* Kre6	65	78
S. cerevisiae Skn1p	*C. albicans* Skn1	59	75

Table 3

Comparison of *C. neoformans* Kre6/Skn1 proteins

Protein 1	Protein 2	% identity	% similarity
C. neoformans Kre6	*C. neoformans* Kre61	58	71
C. neoformans Kre6	*C. neoformans* Kre62	56	70
C. neoformans Kre6	*C. neoformans* Kre63	59	74
C. neoformans Kre6	*C. neoformans* Kre64	45	59
C. neoformans Kre6	*C. neoformans* Skn1	69	81